

# REVIEW OF CLASSICAL DESIGN METHODS AS APPLIED TO ALUMINUM BILLET HEATING WITH INDUCTION COILS

Mark William Kennedy<sup>1</sup>, Shahid Akhtar<sup>1</sup>, Jon Arne Bakken<sup>1</sup>, Ragnhild E. Aune<sup>1,2</sup>

<sup>1</sup>Department of Materials Science and Engineering, Norwegian University of Science and Technology, N-7491 Trondheim,  
NORWAY

<sup>2</sup>Department of Materials Science and Engineering, Royal Institute of Technology, 100 44  
Stockholm,  
SWEDEN

Communicating author: ragnhild.aune@ntnu.no

Keywords: Induction, heating, billet, short coil

## Abstract

In the present study classical induction design tools are applied to the problem of heating non-magnetic metal billets, using 50 Hz AC. As an example of great practical industrial interest, the induction heating of aluminum billets is addressed specifically. The predicted work piece power is compared with the measured work piece power for a long and a short coil, using well established methods, such as those of Burch and Davis, introduced in 1926/28, Dwight and Bagai in 1935, Baker in 1944/57, Vaughan and Williamson in 1945, and by Tudbury in 1960. A calculation methodology based on a combination of the available tools is also introduced and discussed. The method has proven to give an error of <10% of the actual work piece power. An equation for Tudbury's work piece shortness correction factor is disclosed for the first time.

## Introduction

Induction heating of metal billets is a practical problem, with a geometry suitable for solution using analytical methods. This paper will examine solutions related specifically to round work pieces in round coils, although the methods presented can be extended to other regular shapes of work pieces and coils[1]. The methods can also be extended to ferromagnetic materials with slight changes[2-3]. It is assumed that the coil and work piece have a consistent diameter over their entire length and that the work piece is at least as long as the coil. Correction factors can be derived for the cases where the work piece is shorter than the coil.

The study of induction heating by coils began in the late 19<sup>th</sup> century with theoreticians like Heaviside[4]. The work of Burch and Davis[5-7] in the 1920's greatly improved the theoretical understanding of induction applied to metallurgy. Many investigators in the 1930's-1950's: Dwight and Bagai[8], Baker[1-2, 9], Vaughan and Williamson[3, 10] and others[11-12] added to our understanding with clearer mathematics, solutions for specific applications, semi-empirical modifications and practical design tools. Much of the accumulated knowledge is available in books, such as Tudbury's practical text or Simpson's engineering guide from 1960[13-14]. Perhaps the best description and derivation of the theoretical and semi-empirical solutions can be found in Davies[15].

In coreless induction heating, a work piece is placed within an induction coil as shown in Figure 1. Both the work piece and coil can be of arbitrary shape and length. A cyclically varying voltage is impressed upon the coil, which creates a time varying current in the coil and a strong magnetic field along the axis. This varying magnetic field interacts with the work piece to induce circular voltage gradients and “eddy currents,” which circulate around the axis of the coil, but in a direction opposite the coil’s current, as shown in Figure 1. The circulation of the eddy currents,  $J$  ( $A/m^2$ ) and the work piece’s natural resistivity,  $\rho$  ( $ohm \cdot m$ ), combine to generate heat,  $P$  ( $W/m^3$ ). The relationship between the coil current, the magnetic field strength, the induced voltages and currents, is complex and will be discussed in some detail. Due to the relative simplicity we will begin by discussing an empty or “air core” coil.

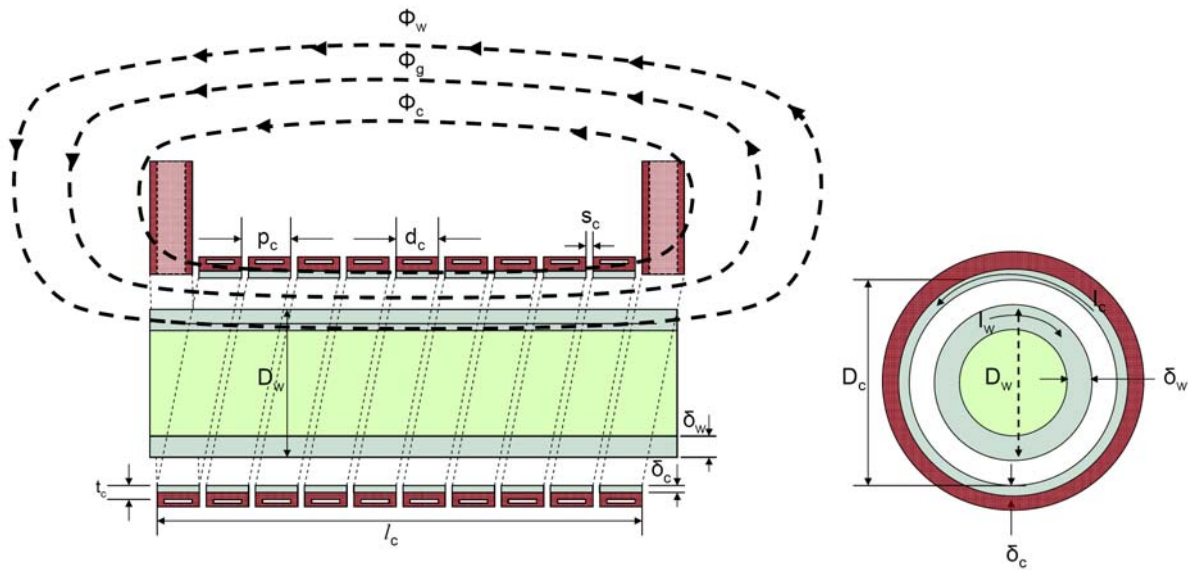


Figure 1. 10 turn induction coil, with billet slightly longer than coil

### Derivation of Coil Impedance and Power Formulae

Let us begin by considering the coil shown in Figure 1. It has a length ( $l_c$ ) that can be measured in two ways: taking the centre-centre distance on the sides of the leads or top-bottom of the coil turns opposite the leads (as shown in Figure 1).

Imagine that the coil was constructed from a solid copper tube of length ( $l_c$ ). Let the thickness of the copper ( $t_c$ ) be very small in comparison with the diameter of the cylinder ( $D_c$ ). ( $N_c-1$ ) grooves of thickness ( $s_c$ ) are cut in a helical spiral along the whole length. This forms a long coil or solenoid, with a geometry approaching that of a theoretical “current sheet” with  $N_c$  turns as shown in Figure 2.

The coil pitch is equal to:

$$p_c = d_c + s_c \quad (1)$$

The coil space factor is the fraction of the side of the coil occupied by copper:

$$k_r = d_c N_c / l_c = d_c N_c / [(N_c - 1) s_c + d_c N_c] \text{ or for large } N_c, k_r \sim d_c / p_c \quad (2)$$

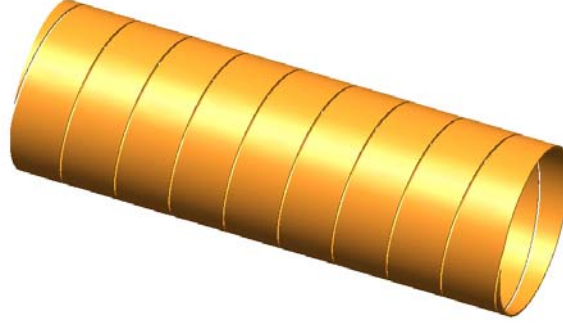


Figure 2. 10 turn helical “current sheet” coil or solenoid

The length of the “wire” in the coil, at the average current depth is:

$$\ell_{\text{wire}} = \pi (D_c + \delta_c) N_c \quad (3)$$

The height of each “wire” is:

$$d_c = \ell_c k_r / N_c \quad (4)$$

We now apply an alternating voltage (AC), at a frequency, which has an electromagnetic penetration depth ( $\delta_c$ ) of much less than the thickness of the conductor in the radial dimension, ( $\delta_c \ll t_c$ ). Where the penetration depth is defined as the depth, which if filled with a homogeneous current (DC current) would yield the same resistance as the AC current distribution over the whole thickness of the conductor. At high frequency, current in a solenoid is biased towards the surface of the wire facing the interior of the coil and attenuates in an exponential manner with each penetration depth into the conductor.

The penetration depth can be calculated from the following commonly accepted formula[16-17]:

$$\delta_c = (2 \rho_c / (\omega \mu_r \mu_o))^{0.5} = (\rho_c / (\pi \mu_r \mu_o f))^{0.5} \quad (5)$$

Where:  $\mu_o$  is the magnetic permeability of free space, ( $4 \pi 10^{-7}$  H/m) and  $\mu_r$  is the relative permeability for copper and aluminum, which is equal to 1.

The angular frequency is:

$$\omega = 2 \pi f \text{ (radians per second)} \quad (6)$$

Where:  $f$  is the frequency (Hz).

A modified penetration depth can be calculated accounting for the presence of the air gaps as derived by Howe[18] and with demonstrated accuracy according to the data of Vaughan and Williamson [10], using the  $k_r$  factor from Equation (2):

$$\delta_c = (2 \rho_c / (k_r \omega \mu_r \mu_o))^{0.5} = (\rho_c / (k_r \pi \mu_r \mu_o f))^{0.5} \quad (7)$$

The alternating current resistance of the coil can then be found using the simple formula:

$$R_c = \rho_c \ell_{\text{wire}} / a_{\text{current}} \quad (8)$$

Where the effective area of the current path for alternating current is:

$$a_{\text{current}} = d_c \delta_c = \delta_c \ell_c k_r / N_c \quad (9)$$

The resistivity of the copper is a function of temperature and composition as shown in Figure 3. Phosphorous deoxidized copper (with up to 0.04 wt% residual P) will have an actual conductivity of about 80% IACS (International Annealed Copper Standard of 1913[19]). 100% IACS is equivalent to a resistivity of 1.7241E-8 ohm·m at 20°C, with copper having a temperature coefficient of 0.00393[19-21].

Actual coil copper resistivity can be estimated by:

$$\rho_c = 1.7241\text{E-}8 \text{ ohm}\cdot\text{m} (1+0.00393 (T_c-20^\circ\text{C})) 100 / \% \text{IACS} \quad (10)$$

We can now estimate using equations (1-10) the AC resistance of the coil to be:

$$R_c = \pi (D_c + \delta_c) N_c \rho_c / (\delta_c \ell_c / N_c) = \pi (D_c + \delta_c) N_c^2 \rho_c / (\delta_c \ell_c k_r) \quad (11)$$

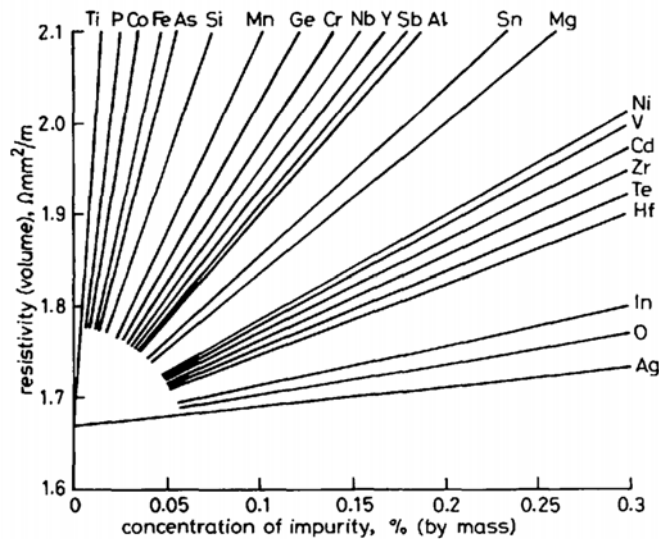


Figure 3. Approximate effect of impurities on the resistivity of copper[20]

Power lost from the coil to the cooling water can then be calculated from  $P=I_c^2 R_c$ , where  $I_c$  is the root mean square (R.M.S.) value:

$$P_c = I_c^2 \pi (D_c + \delta_c) N_c^2 \rho_c / (\delta_c \ell_c k_r) \quad (12)$$

If the electromagnetic penetration depth exceeds more than half the actual conductor thickness, as might occur at low frequency ( $t_c > \delta_c > 0.5 t_c$ ), some small error will be encountered with equations (11-12). If the penetration depth is significantly greater than the thickness ( $\delta_c > t_c$ ), the resistance can be accurately estimated using the total conducting area (equivalent to the DC resistance in this case) in Equation (8). Care must be taken to account for the loss of conducting area due to the cooling channel. In other cases, either an “exact” theoretical solution[18, 22-28] or empirical data[29] must be used. There is a tendency for the “exact” solutions to be in error

for very short coils ( $\ell/D_c < 1$ ), or coils with large spaces between the turns ( $k_r < 0.7$ ). It is best if the coil can be designed such that ( $\delta_c < 0.5t_c$ ), for low resistive losses and accurate design.

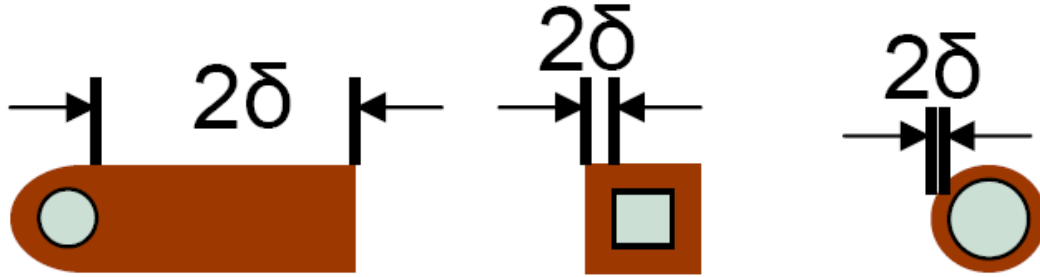


Figure 4. Examples of conductor shapes for mains frequencies (50-60 Hz), medium (500-5000 Hz), and high frequency furnaces, each with the recommended wall thickness of  $2\delta$ [30]

It is standard practice in induction furnace coil design to assume that the coil is magnetically thick ( $\delta_c < 0.5t_c$ ). It is then assumed that the wire of the coil has an internal reactance equal to the resistance, which is the same as saying that the wire has an internal power factor of 0.707:

$$X_c = R_c \quad (13)$$

This is a dubious assumption except for very high ratios of thickness to penetration depth ( $\delta_c < 0.25t_c$ ), but causes little error in the total estimation of reactive power. Errors are smallest at high frequency with thin conductors as shown in Figure 4.

### Magnetic Field, Inductance and Impedance for Short and Long “Air Core” Coils

If we imagine that our coil is merely a section of length  $\ell$  of an infinitely long coil, the magnetic flux density within the coil is independent of position in the coil. The magnetic flux density can then be estimated using either Amperè’s or the Biot-Savart law to be:

$$B_\infty = \mu_0 N_c I_c / \ell \quad (14)$$

This assumes negligible flux density outside of the coil (no reluctance in the external magnetic circuit), ignores end effects (there are no ends to an infinite coil) and assumes complete linking of all the flux with all the turns of the coil.

The inductance of the empty long coil (“air core” inductor) is then determined from the number of flux linkages per unit current:

$$L_\infty = A_c \mu_0 N_c^2 / \ell = A_c N_c B_\infty / I_c \quad (15)$$

Where  $A_c$  is the area of the coil:

$$A_c = \pi (D_c + \delta_c)^2 / 4 \quad (16)$$

For round tubes or if  $\delta_c \geq t_c$ , the diameter at the centre line of the conductor should be used.

Induction furnace coils are nearly always “short coils”,  $\ell_c/(D_c+\delta_c)<8$ , and are often very short  $\ell_c/(D_c+\delta_c)<1$ . There are fundamental differences between long and short coils. In the case of short coils, the assumptions of uniform internal and negligible external flux density are no longer correct. The short coil flux density is now a function of both length and radius [ $B_{\text{short}}(\ell_c, r_c)$ ] and there now exists an external magnetic flux density near the coil, with a finite reluctance. The approximation that all the flux, links all the turns is also questionable.

In the case of short “air core” coils, exact solutions have been calculated for the “end effect” of a “current sheet” and a correction factor ( $k_N$ ) tabulated by Nagaoka[31-32]. The short coil inductance can then be calculated by:

$$L_0 = k_N A_c \mu_0 N_c^2 / \ell_c = k_N A_c N_c B_\infty / I_c \quad (17)$$

Equation (17) is the equivalent to saying that the actual flux density (integrated by length and radius) of the short coil in the axial direction is:

$$B_0 = k_N B_\infty = k_N \mu_0 H_\infty = k_N \mu_0 N_c I_c / \ell_c \quad (18)$$

The Nagaoka factor has been plotted in Figure 5. Alternatively, an empirical equation like that of Wheeler[33], can be used to estimate coil inductance for a short coil. Wheeler’s equation has been reformulated by Knight[34] to give the Nagaoka coefficient directly:

$$k_N = 1/[1 + 0.4502 (D_c + \delta_c) / \ell_c] \quad (20)$$

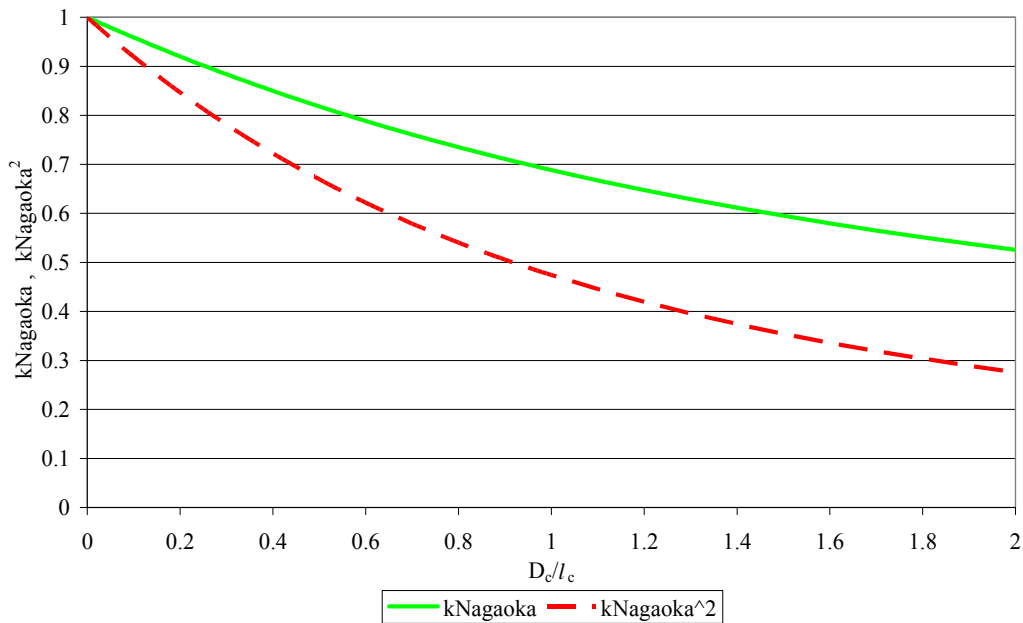


Figure 5. Nagaoka’s short coil correction factor

If round tubing is used, it is necessary to apply a round wire correction such as Rosa’s[32] to the calculated inductance.

Once the inductance of the short coil has been obtained, it is then simple to estimate the inductive reactance ( $X_0$ ), the total coil impedance ( $Z_0$ ) and voltage drop ( $V_0$ ) for the “air core” coil:

$$X_0 = \omega L_0 = 2 \pi f L_0 \quad (21)$$

$$Z_0 = (R_c^2 + X_0^2)^{0.5} \quad (22)$$

$$V_0 = I_0 Z_0 \quad (23)$$

### Impact of the Work Piece on the Magnetic Field

In the presence of a work piece, we can see from Figure 1, that the total magnetic flux can be divided into 3 parts: flux which links only with the coil ( $\Phi_c$ ), flux in the air gap ( $\Phi_g$ ) and the net flux that links the billet ( $\Phi_w$ ). These fluxes in turn produce equivalent inductances and reactive impedances:  $X_c$ ,  $X_g$  and  $X_w'$ , as indicated in the simplified series circuit diagram, Figure 6.

Several things happen to the magnetic field when a work piece is placed into the coil:

1. The “aperture” of the coil is effectively reduced, making the effective diameter to length ratio look smaller, changing the magnitude of the short coil correction factor  $k_N$  and the flux density in the air gap along the axial direction of the coil.
2. Space that was formerly air is occupied by the work piece, reducing the total air gap flux.
3. Eddy currents in the billet produce magnetic fields, which oppose the magnetic field of the coil, reducing the net flux in the space occupied by the billet.

Vaughan and Williamson proposed an empirical modification to the short coil correction factor based on the volumetric fraction of the air-gap occupied by the work piece. Their proposed correction factor is applied to the Nagaoka coefficient to produce an “effective Nagaoka coefficient” for a short coil containing a work piece:

$$k_N^* = k_N (1 - [D_w / D_c]^2) + [D_w / D_c]^2 \quad (24)$$

To be consistent with the previous formulae:

$$k_N^* = k_N (1 - [D_w / (D_c + \delta_c)]^2) + [D_w / (D_c + \delta_c)]^2 \quad (25)$$

The effective magnetic flux density in the air gap of a short coil containing a work piece can then be calculated by:

$$B_0^* = k_N^* \mu_0 H_\infty = k_N^* \mu_0 N_c I_c / \ell_c \quad (26)$$

It is assumed that this magnetic flux density is constant over the width of the air gap, and that it is this flux density, which induces the eddy currents in the work piece.

The contribution of the air gap to the total inductive impedance of the circuit is:

$$X_g = \omega L_g = 2 \pi f A_g N_c B_0^* / I_c = k_N^* \mu_0 N_c^2 \pi^2 (D_c^2 - D_w^2) / 2 \ell_c \quad (27)$$

## Derivation of Work Piece Impedance and Power Formulae

It is difficult to make electrical measurement in the work piece. The effect of the work piece on the circuit is normally inferred from electrical changes in the coil, with and without a work piece. As a first approximation it can be assumed that the resistance and reactance of the coil are not affected by the work piece and all measured electrical changes can be attributed to the work piece and changed air gap.

One approach to the mathematics is to consider the magnetic and electrical circuits to be a series circuit as shown in Figure 6, for a “long coil”. The picture is similar, but more complex for a “short coil” if the reluctance of the external magnetic circuit is to be accounted for explicitly[1].

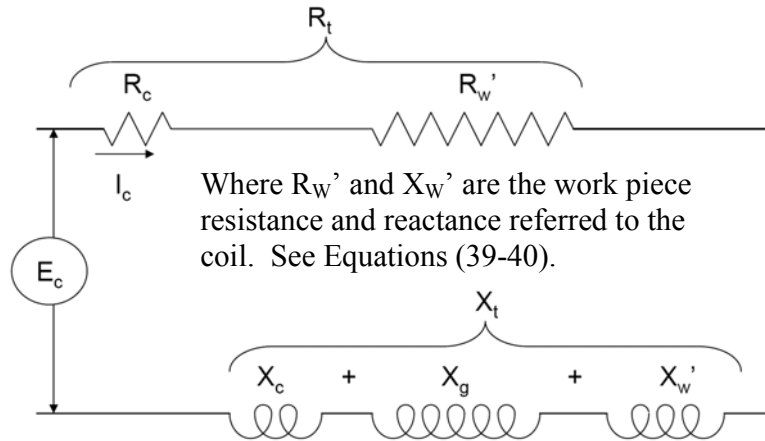


Figure 6. Series equivalent circuit for an induction furnace coil and work piece

When alternating current is applied, the coil and work piece become inductively coupled in a similar way to the windings of a transformer over the length shared by the coil and work piece. The magnetic flux density produced in the air gap by the coil, is the same flux density, which induces eddy currents at the surface of the work piece:

$$B_w = B_0^* = \mu_0 \mu_r N_w I_w / \ell_w = k_N^* \mu_0 N_c I_c / \ell_c \quad (28)$$

If  $\ell_w \geq \ell_c$  take  $\ell_w = \ell_c$ , i.e. it is assumed that only the length of work piece within the coil interacts with the magnetic field of the coil. In the following derivations we take  $\ell_w \geq \ell_c$  and substitute  $\ell_c$  in the place of  $\ell_w$ .

$$N_w I_w = k_N^* N_c I_c (\ell_c / \ell_c) = k_N^* N_c I_c \quad (29)$$

The eddy currents induced in the billet are assumed to make a single turn ( $N_w=1$ ), while the current in the coil makes  $N_c$  turns. It is standard practice to refer conditions in the work piece back to the coil (where we measure the voltage, current, resistance and impedance of the total circuit) via the standard transformer relationship:

$$I_w = k_N^* N_c I_c / 1 = k_N^* N_c I_c \quad (30)$$



By analogy to Equation (11), with  $N_w=1$ ,  $k_r=1$  (as the work piece has no “air gaps”) and the average diameter is **reduced** by the penetration depth:

$$R_w = \pi (D_w - \delta_w) N_w \rho_w / (\delta_w \ell_c / N_w) = \pi (D_w - \delta_w) \rho_w / (\delta_w \ell_c) \quad (31)$$

Where  $\delta_w$  can be calculated using Equation (5) substituting work piece (w) for coil (c) values. *If the work piece is shorter than the coil, the calculated resistance must be corrected by multiplying by the ratio ( $\ell_w / \ell_c$ ).*

Using Equations (30-31), the power in the work piece is then:

$$P_w = I_w^2 R_w = k_N^2 (I_c N_c)^2 R_w = k_N^2 (I_c N_c)^2 \pi (D_w - \delta_w) \rho_w / (\delta_w \ell_c) \quad (32)$$

Equation (32) is sufficiently accurate (about 1% error) provided that  $\xi_w > 3$ :

$$\xi_w = D_w / (\delta_w \sqrt{2}) \quad (33)$$

$\xi_w$  as mentioned above is a very important dimensionless parameter in induction heating theory, and can be found in many different forms in various publications.

The actual resistance in the work piece can be “reflected” back onto the coil via:

$$R_w' = R_w N_c^2 \quad (34)$$

and added to the coil resistance, to give the total circuit resistance as indicated in Figure 6:

$$R_t = R_w' + R_c \quad (35)$$

Higher mathematical precision requires the exact solution to the field equations using complex numbers and involves use of (computationally challenging) Bessel functions[4, 6, 8]:

$$R_w' = [\pi N_c^2 D_w \rho_w / (\delta_w \ell_c)] \sqrt{2} (\text{ber}\xi_w \text{ber}'\xi_w + \text{bei}\xi_w \text{bei}'\xi_w) / [\text{ber}^2(\xi_w) + \text{bei}^2(\xi_w)] \quad (36)$$

Substituting Equation (33) in (36):

$$R_w' = (\sqrt{2} \pi N_c^2 \rho_w \xi_w / \ell_c) \sqrt{2} (\text{ber}\xi_w \text{ber}'\xi_w + \text{bei}\xi_w \text{bei}'\xi_w) / [\text{ber}^2(\xi_w) + \text{bei}^2(\xi_w)] \quad (37)$$

Defining  $\varphi(\xi_w)$ :

$$\varphi(\xi_w) = \sqrt{2} (\text{ber}\xi_w \text{ber}'\xi_w + \text{bei}\xi_w \text{bei}'\xi_w) / [\text{ber}^2(\xi_w) + \text{bei}^2(\xi_w)] \quad (38)$$

Substituting  $\varphi(\xi_w)$  in (37):

$$R_w' = \sqrt{2} \pi N_c^2 \rho_w \xi_w \varphi(\xi_w) / \ell_c \quad (39)$$

Similar solutions exist for the inductive reactance of the work piece[4, 6, 8]:

$$X_w' = \sqrt{2} \pi N_c^2 \rho_w \xi_w \psi(\xi_w) / \ell_c \quad (40)$$

Where  $\psi(\xi_w)$  is defined as:

$$\psi(\xi_w) = \sqrt{2} (\text{ber}'_{\xi_w} \text{bei}'_{\xi_w} - \text{bei}_{\xi_w} \text{ber}'_{\xi_w}) / [\text{ber}^2(\xi_w) + \text{bei}^2(\xi_w)] \quad (41)$$

Substituting Equations (39) and (34) into Equation (32) for the power developed in the work piece:

$$P_w = k_N^{*2} \sqrt{2} \pi (I_c N_c)^2 \rho_w \xi_w \varphi(\xi_w) / \ell \quad (42)$$

And similarly for the reactive power of the work piece:

$$Q_w = k_N^{*2} \sqrt{2} \pi (I_c N_c)^2 \rho_w \xi_w \psi(\xi_w) / \ell \quad (43)$$

$\varphi(\xi_w)$  and  $\psi(\xi_w)$  are plotted in Figure 7 versus  $\xi_w$  for use with Equations (42-43). Baker presents the equations in slightly different format, using his functions P and Q, which are similar solutions for the real and imaginary parts of the Bessel functions[1]. Excellent derivations of Baker's P and Q can be found in the literature[14-15].

The power factor of the work piece can be calculated by:

$$\text{P.F.} = \varphi(\xi_w) / [\varphi(\xi_w)^2 + \psi(\xi_w)^2]^{0.5} \quad (44)$$

and becomes close to constant for  $\xi_w > 3$ , converging slowly towards 0.707 or  $\sqrt{2}/2$ , for very high  $\xi_w$ .

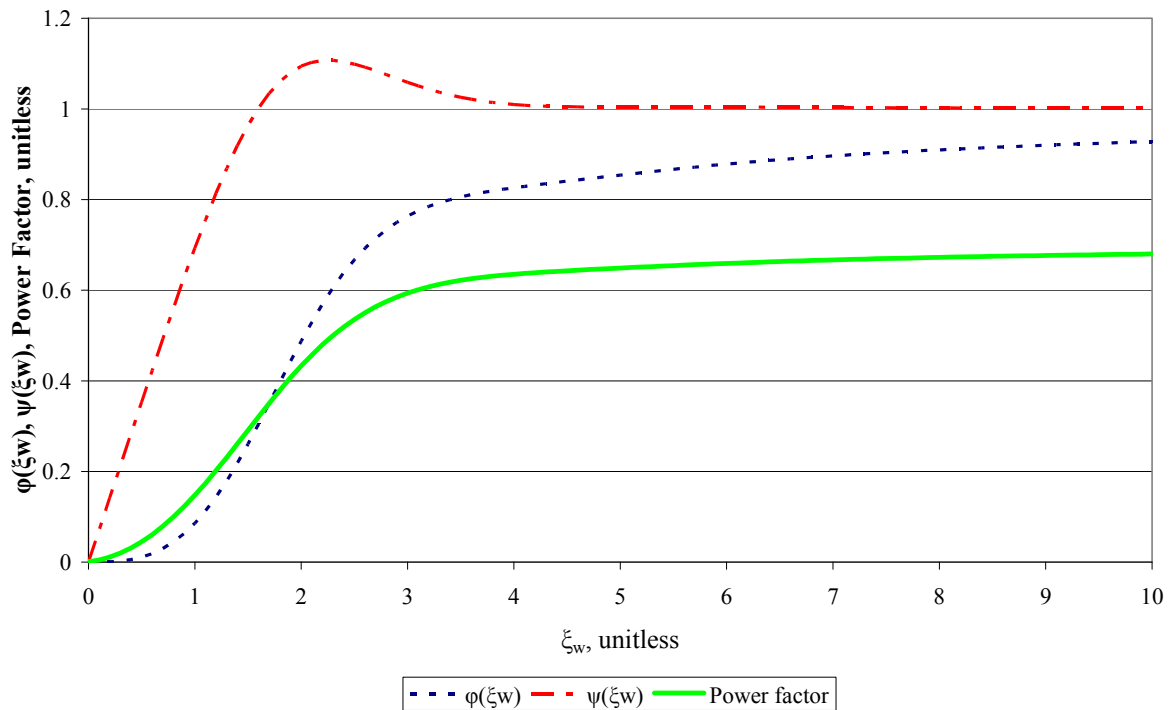


Figure 7. Resistance and Reactive factors for use with Equations (42-43).

## Work Piece Shortness Correction Factor

As the length of a coil increases for a fixed diameter, the Nagaoka coefficient and the modified coefficients  $k_N^*$  and  $k_N^{*2}$  approach unity and the ratio of the coil diameter to length ( $D_c/l_c$ ) approaches zero at the limit. As the diameter of the work piece is reduced with a constant coil diameter, the coil increasingly looks like an “air core” coil, and at the limit of  $D_w/D_c$  going to zero,  $k_N^{*2} = k_N^2$ .

The modified Nagaoka coefficient squared ( $k_N^{*2}$ ) of Vaughan and Williamson[10], is plotted in Figure 8. If this figure is compared with the original graph in the book by Tudbury[13], it is clear that they are identical and that the equation fits the logical tests given above. See Figure 5 for the comparison of  $k_N^2$  with the intercepts on Figure 7 (limit of the “air core”). Tudbury’s original book must be referenced, as later reproductions are not drawn accurately[35].

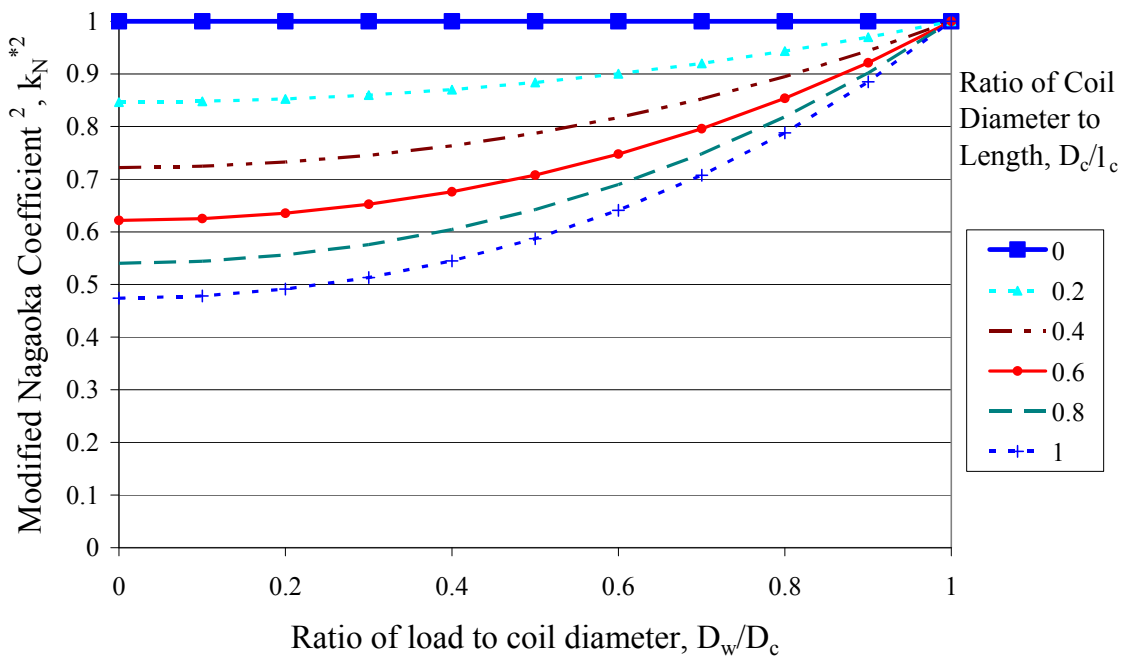


Figure 9. Tudbury’s Work Piece Shortness Factor and Vaughan and Williamson’s modified Nagaoka Coefficient<sup>2</sup>[10, 13]

## Results and Discussion

Experiments were conducted using a number of aluminum billets of different sizes and compositions, using two different coils as indicated in Table I. Billet electrical conductivities were estimated by simultaneously minimizing the error from Equation (42) and Baker's method, while ensuring the conductivity fell within the range of published specifications for each alloy. Coils were constructed using thin wall tubing for convenience (as power efficiency was not an issue), where the AC resistance was identical with the DC resistance ( $\delta_c > d_c > t_c$ ). This eliminated the need to have capacitor banks and reduced the impact of harmonics on the measurements. Copper tubing conductivity was ~80% IACS. Measurements were taken with a Fluke 43B Power Quality Analyzer, equipped with a calibrated Fluke i1000s current probe with an accuracy of 1%.

Work pieces were cooled to below room temperature ( $\sim 10^\circ\text{C}$ ) and then readings were taken before they heated beyond  $30^\circ\text{C}$ , such that  $20^\circ\text{C}$  was a typical temperature to evaluate the resistivity. Ideally the work pieces would have been drilled through, cooled with water to achieve isothermal conditions and the heat input determined calorimetrically; however, in the case of the magnetically thin work pieces (2 and 3) this would have created significant measurement errors. A non-metallic water jacket would be a possible option for cooling without influencing the electromagnetic properties of the work piece.

Table I. Work pieces and coils used in billet heating experiments

Work Pieces:	1	2	3	4	5
Alloy:	A356	6053	6053	6082	7108
Diameter, mm	76.8	38.6	50.5	95.3	95.4
Length, mm	192	356	1078	258	201/340
Resistivity (ohm m) at 20 C:	4.01E-08	4.11E-08	4.11E-08	3.59E-08	3.92E-08
IACS conductivity, %	43	42	42	48	44
Penetration depth (mm) at 50 Hz:	14.25	14.42	14.42	13.49	14.09
$\xi_w$ :	3.810	1.893	2.476	4.996	4.788
$\phi(\xi_w)$ :	0.819	0.397	0.638	0.852	0.846
$\psi(\xi_w)$ :	1.014	1.060	1.104	1.004	1.004
Coil 1	X	X	X	X	X
Coil 2			X	X	X
Coils:					
Coil 1					
Coil 2					
Inside diameter, mm	126	118			
Average diameter, mm	132	124			
Height, mm	111	300			
Coil tube diameter, mm	6	6.35			
Coil tube thickness, mm	1.00	0.762			
Number of turns	16.5	41			
"Aircore" inductance, $\mu\text{H}$	27.6	71.7			
Nagaoka coefficient, Equation (20), $k_N$ :	0.653	0.843			
Resistance at maximum load, ohms	0.0108	0.0319			
Avg. temperature at maximum load, Deg C:	43	62			
Modified Nagaoka coefficient for load 1, $k_N^*$ :	0.771				
Modified Nagaoka coefficient for load 2, $k_N^*$ :	0.683				
Modified Nagaoka coefficient for load 3, $k_N^*$ :	0.704	0.869			
Modified Nagaoka coefficient for load 4, $k_N^*$ :	0.835	0.935			
Modified Nagaoka coefficient for load 5, $k_N^*$ :	0.836	0.935			

Table II. Electrical measurements, coils 1 and 2 with work pieces 1-5

Load Number						Power Factor
	V	A	kVA	kW	kVAR	
1-1	13.14	969	12.7	10.7	7.0	0.84
1-1	14.84	1079	16.0	13.5	8.7	0.84
1-2	13.13	953	12.5	9.8	7.8	0.78
1-2	14.81	1067	15.8	12.5	9.7	0.79
1-3	13.14	954	12.5	10.0	7.6	0.79
1-3	14.81	1067	15.8	12.7	9.5	0.80
1-4	13.13	999	13.1	11.6	6.1	0.88
1-4	14.85	1110	16.5	14.6	7.6	0.89
1-5	13.13	985	13.0	11.4	6.2	0.88
1-5	14.86	1095	16.3	14.4	7.7	0.89
2-3	27.60	703	19.5	16.4	10.5	0.84
2-4	27.58	729	20.1	18.5	7.6	0.93
2-5	27.58	721	19.9	18.5	7.4	0.93

Work piece power has been determined by subtracting the coil power from the power of the work piece and coil and attributing all resistive changes to the work piece. Where multiple readings had been taken, averages are shown in Tables II and III. Measured coil power has been compared to predictions using equations (32) and (42) and against various methods published in the literature[1, 6, 8]. The methods of Vaughan and Williamson[10] and Tudbury[13], utilizing the modified Nagaoka coefficient, will give essentially the same results as Equation (42). Short coil methods of Baker[1] and Burch and Davis[6] and the long coil method of Dwight and Bagai[8], are shown in Table III for comparison.

Table III. Comparison of real and calculated work piece power by various methods

Load Number	Measured Power, W	Equation (32)	Equation (42)	Baker Short Coil	Burch and Davis	Dwight and Bagai
1-1	692	754	759	577	821	1275
1-1	899	936	942	716	1013	1583
1-2	138	224	142	125	271	305
1-2	177	281	178	157	340	382
1-3	325	356	318	266	517	641
1-3	377	445	398	333	647	802
1-4	990	1165	1155	862	945	1656
1-4	1264	1438	1426	1064	1167	2045
1-5	1086	1176	1168	866	962	1673
1-5	1422	1454	1443	1070	1188	2067
2-3	640	674	602	569	740	798
2-4	1553	1533	1520	1591	1402	1738
2-5	1923	1810	1797	1627	1657	2054
Error	+/-~2%	16.6	6.0	14.6	33.0	67.6

It can be seen in Table III, that Equation (42) produces the best results in comparison with the measured data, with a typical error of 6% and a maximum error of 16%. Except for work piece number 2 with  $\xi_w < 3$ , Equation (32) gave comparable results with those of Equation (42).

Coil 1 had a length/diameter ratio of 0.84 using the average diameter. While coil 2 had a ratio of 2.42, i.e. coil 2 was relatively long, while coil 1 was quite short. It can be seen in Table III that the use of the modified Nagaoka coefficient gave an excellent correction for coil shortness, such that the calculation errors are comparable for both coils using equations (32) and (42). Baker's method gives reasonable, but less accurate results for all work pieces and coils. Burch and Davis' short coil correction does not work well for small  $D_w/D_c$  (work pieces 2 and 3). Dwight and Bagai's long coil method is of course only suitable for the "long" coil number 2.

Please note that for coil 2, work piece 4 was shorter than the coil and that the suggested correction factor of Baker[1] was applied to all methods, i.e. the calculated resistance of the work piece, e.g. Equation (31), was multiplied by the ratio of the length of the work piece/length of the coil ( $l_w/l_c$ ). This is a direct consequence of Equation (28).

## Conclusions

A method has been described using a modified Nagaoka coefficient, capable of estimating work piece power to better than 10% accuracy, for long and short coils, including cases where the work piece is shorter than the coil. Tudbury's work piece shortness factor has been found to be the square of the modified Nagaoka coefficient as proposed by Vaughan and Williamson in 1945. Given that the presence of a work piece has now been shown to change the magnetic field inside the air gap of a short coil significantly, the assumption that the impedance of the coil does not change due to the presence of the work piece can be questioned. It would be of value to directly measure electrical conditions in the work piece, e.g. circular voltage gradients, in order to separate the effect of the coil on the work piece and the work piece on the coil.

## Acknowledgements

The authors wish to express their gratitude to Egil Torsetnes at NTNU, Trondheim, Norway, for helping with the design and construction of the experimental apparatus. Deepest gratitude is also due to Kurt Sandaunet at Sintef, Trondheim, Norway, for the use of the Sintef laboratory and his contribution in the execution of the experiments. Special thanks to Liss Pedersen at Alcoa, Lista, Norway, for the supply of filter materials. The author would also like to acknowledge the funding from the Norwegian Research Council through the RIRA project.

## References

1. R. Baker, "Design and calculation of induction heating coils'," *AIEE Trans*, 57, (1957), 31-40.
2. R. Baker, "Induction Heating of Moving Magnetic Strip," *American Institute of Electrical Engineers, Transactions of the*, 64, (1945), 184-189.
3. J. Vaughan and J. Williamson, "Design of Induction Heating Coils for Cylindrical Magnetic Loads," *American Institute of Electrical Engineers, Transactions of the*, 65, (1946), 887-892.
4. O. Heaviside, *Electrical Papers*. (London: Macmillan & Co., 1892), 353-416.
5. C. Burch and N. Davis, "LXX. On the quantitative theory of induction heating," *Philosophical Magazine Series 7*, 1, (1926), 768-783.
6. C. Burch and N. Davis, *An introduction to the theory of eddy-current heating*. (London: E. Benn Limited, 1928).
7. C. Burch and N. Ryland Davis, "Über eisenlose Induktionsöfen," *Electrical Engineering (Archiv für Elektrotechnik)*, 20, (1928), 211-223.
8. H. Dwight and M. Bagai, "Calculations for coreless induction furnaces," *American Institute of Electrical Engineers, Transactions of the*, 54, (1935), 312-315.
9. R. Baker, "Heating of Nonmagnetic Electric Conductors by Magnetic Induction---Longitudinal Flux," *American Institute of Electrical Engineers, Transactions of the*, 63, (1944), 273-278.
10. J. Vaughan and J. Williamson, "Design of Induction-Heating Coils for Cylindrical Nonmagnetic Loads," *American Institute of Electrical Engineers, Transactions of the*, 64, (1945), 587-592.
11. H. Storm, "Surface Heating by Induction," *American Institute of Electrical Engineers, Transactions of the*, 63, (1944), 749-755.
12. N. Stansel, "Induction Heating---Selection of Frequency," *American Institute of Electrical Engineers, Transactions of the*, 63, (1944), 755-759.
13. C. Tudbury, *Basics of Induction Heating Vol. 1*, (New York: John F. Rider, 1960).
14. P. Simpson, *Induction heating: coil and system design*. (New York, Toronto, London: McGraw-Hill, 1960).
15. E. J. Davies, *Conduction and induction heating*. (London: Peter Peregrinus on behalf of the Institution of Electrical Engineers, 1990).
16. L. Kelvin, *Mathematical Papers, Vol. 3*, (London: Cambridge University Press, 1890), 484-515.
17. O. Heaviside, *Electrical Papers, Vol. 2*, (London: Macmillan & Co., 1892), 396-424.
18. G. Howe, "The high-frequency resistance of wires and coils," *Electrical Engineers, Journal of the Institution of*, 58, (1920), 152-162.
19. *Copper Wire Tables Circular No. 31*: US Bureau of Standards, 1913).
20. V. Callcut, "Coppers for electrical purposes," *IEE Proceedings A Physical Science, Measurement and Instrumentation, Management and Education, Reviews*, 133, (1986), 174-201.
21. H. Coppers, "Copper Development Association," Orchard House, Mutton Lane, Potters Bar, Herts EN6 3AP, (1990).
22. C. Hickman, "Alternating-Current Resistance and Inductance of Single Layer Coils," *Scientific Papers of the Bureau of Standards, No. 472*, (1923), 73-105.
23. S. Butterworth, "Eddy-current losses in cylindrical conductors, with special applications to the alternating current resistances of short coils," *Philosophical Transactions of the Royal Society of London. Series A, Containing Papers of a Mathematical or Physical Character*, 222, (1922), 57-100.
24. S. Butterworth, "Note on the Alternating Current Resistance of Single Layer Coils," *Physical Review*, 23, (1924), 752-755.

25. S. Butterworth, "On the alternating current resistance of solenoidal coils," *Proceedings of the Royal Society of London. Series A*, 107, (1925), 693.
26. A. Arnold, "The resistance of round-wire single-layer inductance coils," *Proceedings of the IEE-Part IV: Institution Monographs*, 98, (1951), 94-100.
27. A. Reatti and M. Kazimierczuk, "Comparison of various methods for calculating the AC resistance of inductors," *IEEE Transactions on Magnetics*, 38, (2002), 1512-1518.
28. E. Fraga, *et al.*, "Practical model and calculation of AC resistance of long solenoids," *IEEE Transactions on Magnetics*, 34, (1998), 205-212.
29. R. Medhurst, "High Frequency Resistance and Self-Capacitance of Single-Layer Solenoids," ed. *Wireless Engineer*: February, (1947), 35-43.
30. O. Todnem, "Induksjonsoppvarming, Industriell Elektrovarme," ed: NTNU, 1992, 1-60.
31. H. Nagaoka, "The inductance coefficients of solenoids," *Journal of the College of Science*, 27, (1909), 18-33.
32. E. B. Rosa and F. Grover, "Formulas and Tables for the Calculation of Mutual and Self Induction," *Scientific Papers of the Bureau of Standards*, No. 169., (1916), 5-231.
33. H. Wheeler, "Simple inductance formulas for radio coils," *Proceedings of the IRE*, 16, (1928), 1398-1400.
34. D. Knight. (2010, August 25). *3.1. Solenoids: Part 1.*, [http://www.g3ynh.info/zdocs/magnetics/part\\_1.html](http://www.g3ynh.info/zdocs/magnetics/part_1.html)
35. S. Zinn and S. Semiatin, *Elements of induction heating: design, control, and applications*: Asm Intl, 1988), 22.